Genomics 101 (2013) 101–112

Contents lists available at SciVerse ScienceDirect

Genomics

journal homepage: www.elsevier.com/locate/ygeno

Neutrophils infected with highly virulent influenza H3N2 virus exhibit augmented early cell death and rapid induction of type I interferon signaling pathways

Fransiskus X. Ivan [a], K.S. Tan [b], M.C. Phoon [b], Bevin P. Engelward [c], Roy E. Welsch [c], Jagath C. Rajapakse [d], Vincent T. Chow [b,*]

[a] Computation and Systems Biology Program, Singapore-MIT Alliance, Singapore
[b] Infectious Diseases Program, Department of Microbiology, Yong Loo Lin School of Medicine, National University Health System, National University of Singapore, Kent Ridge, Singapore
[c] Massachusetts Institute of Technology, Cambridge, MA, USA
[d] BioInformatics Research Centre, Nanyang Technological University, Singapore

ARTICLE INFO

Article history:
Received 14 September 2012
Accepted 17 November 2012
Available online 27 November 2012

Keywords:
Virulent influenza virus
Neutrophils
Apoptosis
Type I interferon signaling

ABSTRACT

We developed a model of influenza virus infection of neutrophils by inducing differentiation of the MPRO promyelocytic cell line. After 5 days of differentiation, about 20–30% of mature neutrophils could be detected. Only a fraction of neutrophils were infected by highly virulent influenza (HVI) virus, but were unable to support active viral replication compared with MDCK cells. HVI infection of neutrophils augmented early and late apoptosis as indicated by annexin V and TUNEL assays. Comparison between the global transcriptomic responses of neutrophils to HVI and low virulent influenza (LVI) revealed that the IFN regulatory factor and IFN signaling pathways were the most significantly overrepresented pathways, with activation of related genes in HVI as early as 3 h. Relatively consistent results were obtained by real-time RT-PCR of selected genes associated with the type I IFN pathway. Early after HVI infection, comparatively enhanced expression of apoptosis-related genes was also elicited.

1. Introduction

Highly virulent influenza (HVI) infection is characterized by dysregulated innate immune responses in various influenza animal models, including our murine model using mouse-adapted HVI H3N2 virus [1]. These include excessive expression of type I interferon (IFN) stimulated genes, as well as cytokines and chemokines early after infection. Furthermore, analyses of bronchoalveolar lavage from animals infected with HVI viruses reveal significantly increased cellularity and numbers of neutrophils and macrophages in their lungs compared to those infected with low virulent influenza (LVI) viruses [2]. It is therefore logical to investigate the global transciptomic responses of these two innate immune cell types following infection with influenza viruses of varying virulence, and to elucidate their contributions to differential lung pathogenesis.

Lee et al. [3] compared the transcriptional profiles of primary human macrophages infected by LVI and HVI viruses, i.e. seasonal H1N1 and avian H5N1, respectively. Highly pathogenic H5N1 induces robust expression of proinflammatory cytokine/chemokine and type I IFN-related genes, including CXCL10 and IFNβ1. In contrast, murine alveolar macrophages fail to express strong IFN and cytokine expression in response to lethal H1N1 PR8 influenza virus infection [4]. These opposing results may be attributed to the ability of H5N1 virus to replicate in human alveolar macrophages, but not the pandemic swine origin H1N1-2009 virus [5]. Thus, the contribution of macrophages to the dysregulation of innate immune responses following influenza infection appears to be strain-specific, and merits further investigations.

There has been hitherto no transcriptomic study that specifically investigates the differential effects of HVI and LVI virus infections of neutrophils. However, the role of neutrophils during *in vivo* infection with influenza virus of varying virulence has been investigated by comparing infection of control animals versus those animals whose neutrophils are specifically depleted with monoclonal antibody 1A8. Tate et al. [6] demonstrated that neutrophils are particularly beneficial in controlling viral replication in animals infected with intermediate or highly virulent viruses, whereas the absence of neutrophils in animals infected with LVI virus does not affect the course of the disease. We have previously reported that PR8 virus-infected, neutrophil-depleted animals display fewer clinical signs and milder pathologic changes compared to infected, macrophage-depleted animals that exhibit respiratory distress and enhanced acute lung injury [7], suggesting that neutrophils mediate greater lung damage than macrophages. Hence, neutrophils may also contribute to the dysregulation of innate immunity, cytokine storm, and severe lung injury.

Several characteristics of influenza virus infection of neutrophils have been elucidated. The viral hemagglutinin activates an atypical

* Corresponding author at: Infectious Diseases Program, Department of Microbiology, Yong Loo Lin School of Medicine, National University Health System, National University of Singapore, 5 Science Drive 2, Kent Ridge117597, Singapore. Fax: +65 6776 6872.
E-mail address: micctk@nus.edu.sg (V.T. Chow).

0888-7543/$ – see front matter © 2012 Elsevier Inc. All rights reserved.
http://dx.doi.org/10.1016/j.ygeno.2012.11.008

respiratory burst, where hydrogen peroxide is produced in the absence of detectable superoxide, and subsequently depresses neutrophil functions in terms of chemotaxis, degranulation, and bacterial killing [8]. Furthermore, the nature of influenza infection in neutrophils is abortive, such that viral proteins can be synthesized but new virus progeny is not formed [9]. Influenza virus enhances the surface expression of toll-like receptors (TLRs), including TLR2, TLR7 and TLR8 [10,11], leading to increased respiratory burst, cytokine and chemokine expression in neutrophils. These TLRs may work in conjunction with TREM1 to amplify cytokine expression in neutrophils and macrophages, as revealed by our previous microarray analyses [1]. Influenza virus can also induce higher rates of cell death and apoptosis in neutrophils [12].

The lack of understanding on the direct implications of increased virulence of influenza virus in neutrophils motivated our investigation of global neutrophil responses to LVI and HVI. This study was also driven by our previous findings [1], where genes and pathways associated with neutrophil activities, e.g. neutrophil chemoattractant CXCL1 and TREM1 signaling, were differentially regulated in LVI and HVI. Neutrophils isolated from mouse blood or bone marrow are not ideal since neutrophils are terminally differentiated and naturally die within 1–2 days. However, there are several neutrophil progenitor cell lines that can be differentiated into neutrophils, including MPRO and EML. Neutrophils differentiated from these two cell lines have similar properties to normal neutrophils in terms of chemotaxis, respiratory burst and phagocytosis [13]. Furthermore, these neutrophils are able to release neutrophil extracellular traps (NETs) [14], an antimicrobial mechanism that is also employed by mouse neutrophils [15]. The ability to release NETs implies the full functionality of neutrophils derived from MPRO or EML cell lines.

In this study, the MPRO cell line was induced to differentiate into neutrophils to explore the interactions between neutrophils and H3N2 influenza virus strains of varying virulence. We induced MPRO differentiation to determine the optimal yield and time for infecting neutrophils. Next, we investigated the ability of influenza virus to infect and replicate within these neutrophils, including their apoptotic responses. This neutrophil infection model was also tested using HVI virus propagated in MDCK cells, designated as "MPI" virus. Following validation of the infection model, we performed gene microarray experiments on neutrophils infected with LVI, HVI and MPI viruses. Taken together, our results on the differential transcriptomic responses of neutrophils to these infections provided novel insights into the contribution of neutrophils in accelerating early innate immune responses and apoptosis, especially during HVI infection.

2. Results

2.1. The MPRO cell line differentiates into a significant proportion of mature neutrophils within five days of culture

Two approaches for maintaining neutrophils were compared, i.e. with excess and limited supply of medium. Overall, both approaches generally resulted in similar neutrophil yields, and flow cytometry revealed no significant difference in the proportions of Ly6G-positive neutrophils on days 4, 5 and 6 of differentiation (data not shown).

Considering the senescence of neutrophils with prolonged maintenance, neutrophils were mainly harvested for experiments on day 5 after differentiation, where Ly6G-positivity by flow cytometry was ~20% while the average percentage of neutrophil-like cells estimated by manual or automated counting of Giemsa-stained cells was ~30%. The relatively higher estimates by the latter technique may be attributed to the subjectivity of interpreting the maturation of neutrophils. To explain the different results between Giemsa staining and Ly6G detection by flow cytometry, we also performed flow cytometry using an antibody against granulocyte receptor 1 (Gr-1), also known as RB6-8C5. Unlike monoclonal antibody 1A8 that specifically recognizes Ly6G expressed only in mature neutrophils, Gr-1 recognizes both Ly6G and Ly6C [16,17]. Among neutrophils on day 5, the percentage (average of quadruplicates) of Gr-1-positive cells (32%) was higher than Ly6G-positive cells (18%). Thus, Giemsa staining appeared to be closer to flow cytometry based on Gr-1 staining. As expected, double staining revealed that cells strongly positive for Ly6G were mainly also strongly positive for Gr-1 (data not shown). Finally, there was a population of cells with intermediate Gr-1 but low Ly6G staining that may represent immature neutrophils (or eosinophils to a lesser extent).

2.2. Neutrophils are infectable by influenza virus

The replication rates of HVI and MPI viruses in MDCK cells were significantly higher than that of LVI (Fig. 1). Hence, we focused on MPI, and addressed whether MPI virus is able to infect mature and immature neutrophils. Influenza virus was labeled with a fluorescent lipophilic dye, i.e. 1,1′-dioctadecyl-3,3,3′,3′-tetramethyl-indodicarbocyanine (DiD), to evaluate the percentage of neutrophils being infected. Using 10^6 cells in 200 μl, flow cytometry detected about 4% and 11% of infected cells (average of quadruplicates) after 1 h incubation with influenza virus at multiplicity of infection (MOI) of 0.1 and 1, respectively. Cells positive for DiD staining could still be detected at 24 h post-infection (p.i.). Furthermore, DiD-labeling of influenza virus indicated that both Ly6G-positive and Ly6G-negative (i.e. mature and immature) neutrophils could be infected (data not shown). Finally, 1 h after incubation, confocal microscopy could visualize infected neutrophils with DiD dye clearly dispersed in the cytoplasm (Fig. 2).

2.3. Neutrophils do not support active influenza virus replication

MPI virus titers in supernatants of infected neutrophils at various time-points remained relatively unchanged, but were significantly increased in supernatants collected from infected MDCK cells as positive control (Fig. 3A).

Representative immunofluorescence staining of infected neutrophils at 9 h p.i. using antibody raised against H3N2 virus indicated that viral proteins were synthesized in the cytoplasm as well as nucleus (Fig. 3B). Interestingly, the percentage of neutrophils positive for viral staining was very low at 6 h p.i. (less than 1%), but modestly increased from ~2.5% at 9 h p.i. to 5.5% at 24 h p.i. (Fig. 3C). Taken together, these findings suggest that influenza virus infection of neutrophils is abortive, i.e. the virus does not actively replicate within neutrophils, although viral proteins can be synthesized.

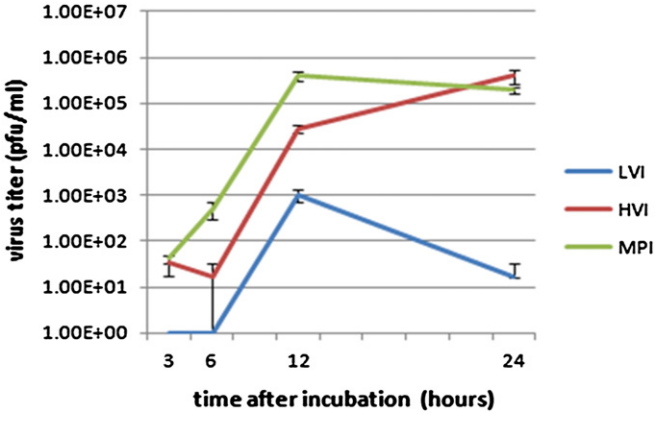

Fig. 1. Comparison between viral replication kinetics of LVI, HVI, and MPI viruses in MDCK cells.

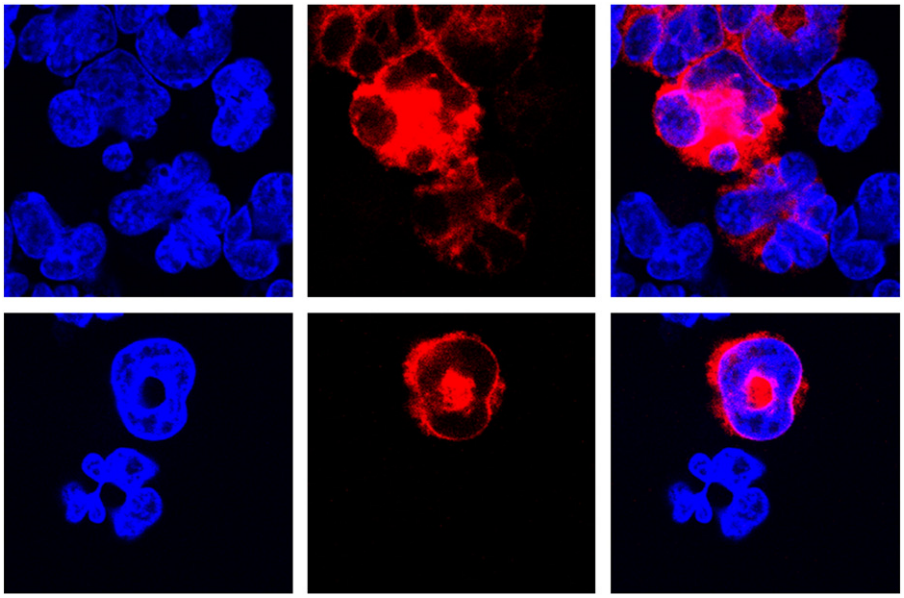

Fig. 2. Confocal microscopy of neutrophils examined 1 h after incubation with DiD-labeled MPI virus. Two representative examples are depicted: the left panels show nuclei stained with DAPI (blue), middle panels exhibit the cytoplasm of infected cells containing DiD label (red), while right panels are the merged images.

2.4. Influenza virus infection of neutrophils augments early and late apoptosis

The effects of MPI virus infection on neutrophil cell death and apoptosis were assessed by flow cytometry based on annexin V (A5) and propidium iodide (PI) staining. This assay determines the proportions of viable cells ($A5^-PI^-$ cells), and of cells undergoing early apoptosis ($A5^+PI^-$ cells). Cell viability of infected neutrophils was generally lower than that of uninfected samples, significantly at 6, 12 and 24 h p.i. Furthermore, the proportion of infected neutrophils undergoing early apoptosis was significantly greater than in uninfected samples from 6 h p.i. onwards (Fig. 4A). In addition, the TUNEL assay indicated a significantly higher percentage of apoptotic cells in infected samples (Fig. 4B). Thus, influenza virus infection accelerates neutrophil death and apoptosis.

2.5. Differential transcriptomic profiles of neutrophils in response to MPI, HVI and LVI

To investigate global transcriptional responses of neutrophils to H3N2 virus, gene expression data were obtained at 3 and 9 h p.i. from neutrophils mock-infected with mouse lung homogenate (control), and infected with LVI, HVI and MPI viruses. Normalized expression data were analyzed by two-way ANOVA with Benjamini–Hochberg correction for multiple tests to identify genes with significant infection, time, and interaction effects. Using a significance level of 0.05 for adjusted p-value, we identified 133 genes with significant infection effect, 4463 genes with significant time effect, and 138 genes with significant interaction between infection and time effects. The overlap between these significant groups of genes is depicted in Fig. 5A.

We focused mainly on the expression profiles of 129 genes that revealed a significant infection effect with an absolute log fold change relative to mock infection of >0.6 at any time-point of any treatment (referred to as differentially expressed genes) as shown in Fig. 5B. The most striking result was that neutrophils responded to HVI more rapidly than to LVI and MPI. In particular, many genes were upregulated as early as 3 h p.i. with HVI, whereas their enhanced expression was only observed at 9 h p.i. for LVI and MPI. Interestingly, the maximal expression changes for most genes in all infections were quite comparable even though the MOI for MPI was ten-fold higher than that for LVI and HVI. Notably, more intense expression changes in response to MPI coincided with relatively higher viral protein synthesis detected at 9 h p.i. as described earlier, whereas only very few neutrophils infected with LVI virus were positive for viral protein staining at this time-point (data not shown).

2.6. Earlier and stronger type I IFN response characterizes HVI infection of neutrophils

Ingenuity Pathway Analysis revealed activation of IFN regulatory factor (IRF) and IFN signaling pathways as the two most significantly overrepresented pathways. The most interesting sub-network in these pathways was that associated with type I IFNβ since this gene, but not type I IFNα and type II IFNγ, was differentially expressed in our microarray data. In addition, FuncAssociate 2.0 listed "cellular response to IFNβ" as the most overrepresented Gene Ontology category. Fig. 5C depicts the heatmap summarizing the expression changes of mainly type I IFN-inducible genes. It is notable that the expression of most IFN-related genes in HVI was more intense at 3 h p.i. compared to that at 9 h p.i., while the reverse pattern was true for LVI and MPI. Fig. 6 illustrates the sub-network associated with IFNβ and highlights: (1) the role of two RNA-sensing molecules RIG-I (DDX58) and MDA5 (IFIH1) in activating IRF3 and IRF7 to induce IFNβ expression and initiate antiviral innate immunity; and (2) the role of IFNβ signaling in elevating the expression of IRF7 and antiviral genes via activation of STAT1, STAT2, and IRF9 complex.

To validate the microarray data, we performed quantitative RT-PCR for several IFN-related genes, including DDX58, IFIH1, IFNβ1, IRF1, IRF7, IRF9, STAT1, STAT2, ISG15, ISG20, IFIT3, OASL2, and CXCL10 (Fig. 7). For several of these genes, i.e. DDX58, STAT2, ISG15, ISG20, OASL2, and CXCL10, there was high correlation between microarray and RT-PCR data (0.96, 0.90, 0.86, 0.93, 0.95, and 0.95, respectively). For all infections, RT-PCR detected overexpression of IRF1 especially at 3 h p.i., and of IRF7 and IRF9 later at 9 h p.i. Furthermore, RT-PCR also indicated early induction of DDX58, STAT1, STAT2, ISG15, ISG20, and OASL2 genes particularly for HVI. The IFNβ1 gene was overexpressed in MPI, LVI, and HVI infections. Overall, there was generally good consistency between RT-PCR and microarray data, with both approaches providing evidence for earlier expression of type I IFN-inducible genes in neutrophils infected with HVI compared to LVI and MPI.

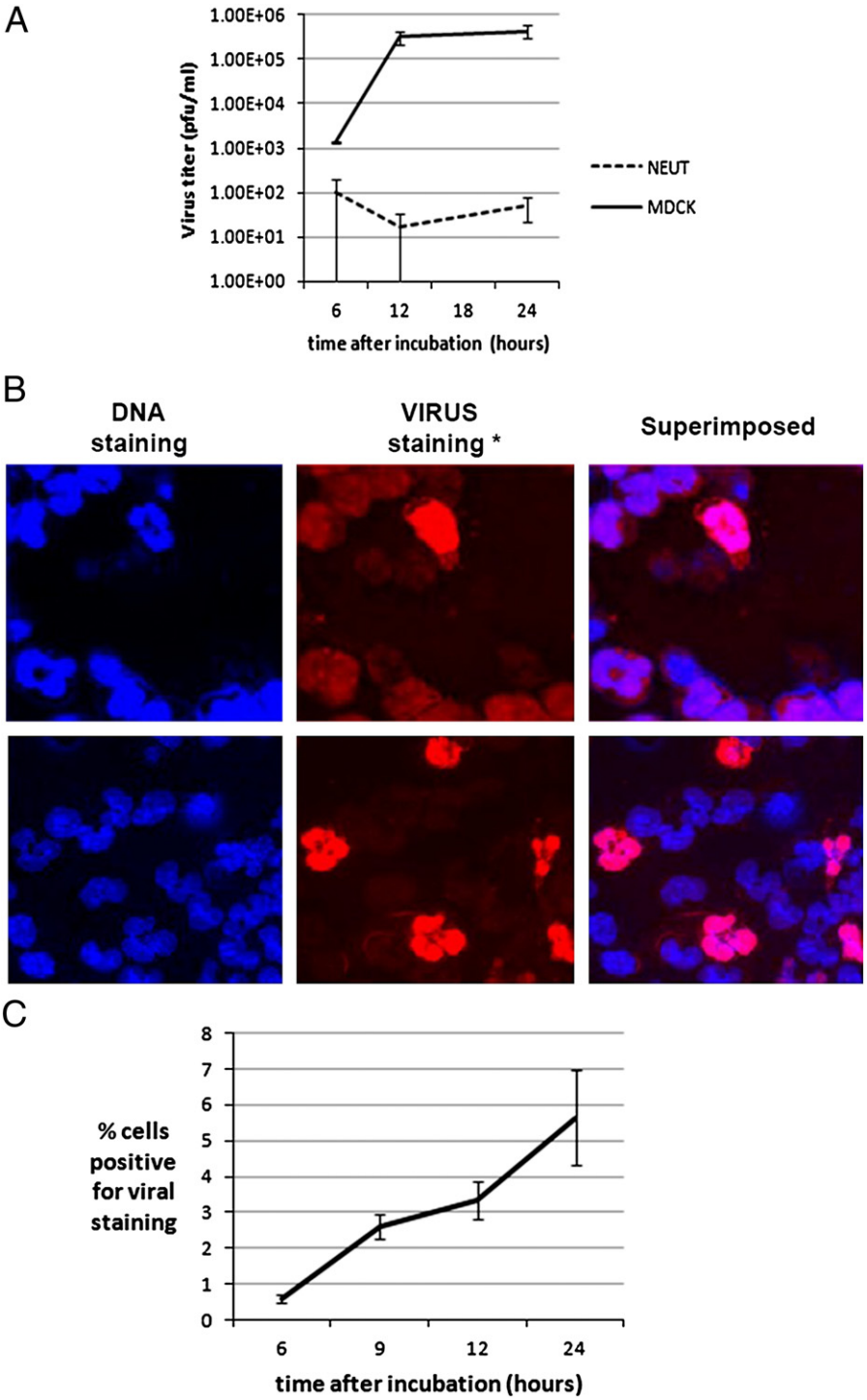

Fig. 3. (A) Comparison of MPI virus titers of supernatants from infected MDCK cells and neutrophils (NEUT). Samples were collected at various time-points after infection at MOI of 0.1. (B) Detection of viral protein synthesis via immunofluorescence staining using polyclonal antibody against H3N2 virus. Viral proteins could be observed in the cytoplasm and/or nucleus of neutrophils at 9 h after incubation with MPI virus. (C) Kinetics of viral protein synthesis based on the percentage of cells positive for viral staining. About 5×10^6 cells per ml were initially infected with MPI virus at MOI of 1.

2.7. Expression of apoptosis genes during MPI, LVI and HVI infections

Microarray data also elucidated higher expression levels of genes associated with apoptotic activity in infected versus uninfected neutrophils, including CASP4, EIF2AK2, NOD1, XAF1, and genes related to retinoic acid-mediated apoptosis signaling, i.e. PARP9, PARP10, and PARP14. It should be emphasized that increased expression of these genes occurred earlier at 3 h p.i. with HVI, in comparison with 9 h p.i. for LVI and MPI infections (Table 1). Specifically for MPI infection, elevated expression of these genes was concomitant with the enhanced apoptosis observed in infected neutrophils.

3. Discussion

We succeeded in employing the MPRO cell line in suspension culture as a source for deriving highly viable neutrophils with a significant proportion of relatively pure neutrophils. Despite evidence to show no differences in the neutrophil yields obtained by using

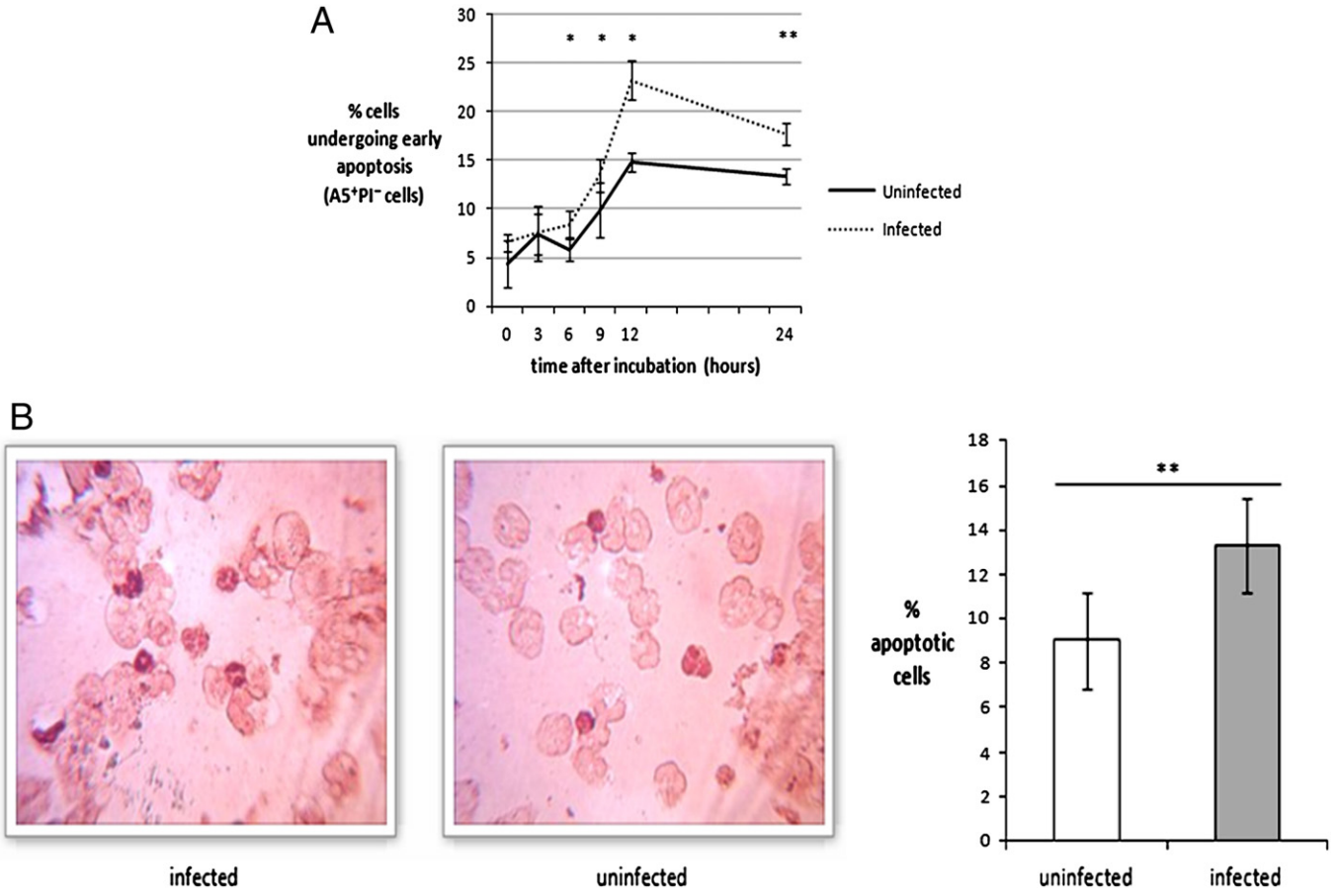

Fig. 4. Induction of enhanced apoptosis in neutrophils infected by influenza virus. About 5×10^6 cells per ml were initially infected with MPI virus at MOI of 1, and compared with uninfected cells. (A) Flow cytometry based on annexin V (A5) and propidium iodide (PI) staining indicated that the proportions of infected cells undergoing early apoptosis (A5-positive and PI-negative) were significantly higher than uninfected cells at multiple time-points. (B) TUNEL assay also revealed augmented apoptosis of infected neutrophils at 12 h p.i., as illustrated by representative images, and quantification of TUNEL-positive cells. The differences between the percentages of infected and uninfected samples were tested using the one-tail paired t-test (* $p<0.05$, ** $p<0.01$).

excess or limited maintenance medium, further experiments may be carried out to optimize neutrophil yield with retinoids to stimulate MPRO differentiation [18]. A neutrophil yield of about 15–20% was determined by Ly6G-based flow cytometry at days 4–6 after differentiation. Examination of Giemsa-stained neutrophils manually or using an automated image analysis system revealed neutrophil yields of about 15–40%.

We demonstrated the potential of the MPRO cell line for modeling influenza virus infection of neutrophils, to gain novel insights into the relationships and interactions between influenza viral virulence and neutrophils. In particular, we showed that influenza virus was able to infect neutrophils by successfully labeling with DiD for tracking the virus in living cells [19]. Notwithstanding that mature and immature neutrophils could be infected, influenza infection in neutrophils was abortive and induced apoptosis. Of interest, we revealed that neutrophils infected with LVI and HVI viruses elicited mainly type I IFN responses, but with differences in kinetics.

Typically, type I and type II IFNs confer protection against viruses and bacteria, respectively. The protective function of type II IFNγ produced by mature and immature neutrophils early after infection has been demonstrated in infection models of *Listeria monocytogenes* [20] and *Streptococcus pyogenes* [21]. However, the protective role of type I IFNα/β produced by neutrophils remains unclear. Despite their potent antiviral and antibacterial activities, overactivation of type I and II IFNs may also be detrimental. Repetitive exposure to inhaled particulate antigens causes overactivation of neutrophil IFNγ that contributes to the pathogenesis of hypersensitivity pneumonitis [22]. Chromatin induces neutrophils to produce IFNα [23], while IFNα can prime neutrophils to release NETs [24], suggesting a feedback loop that may cause overactivation of IFNα, and increase the abundance of NETs. The protective role of IFNβ produced by neutrophils, or the detrimental effects related to its over- or under-activation are not completely understood. For example, overactivation of genes downstream of IFNα/β in neutrophils may contribute to the pathogenesis of tuberculosis [25].

Our infection model of neutrophils with HVI revealed rapid activation of mostly type I IFN-related genes, including the ubiquitin-like modifier ISG15, an antiviral gene that was noticeably highly expressed at 12 h after HVI virus infection of mice [1]. However, not all type I IFN-inducible genes were differentially expressed in influenza infection of neutrophils. For example, we did not observe any change in expression of the MX1 gene, which is implicated in many *in vitro* and *in vivo* influenza models, and determines the effectiveness of type I IFN against influenza virus [26]. Nevertheless, the rapid IFN response in neutrophils may represent a potent contributor to the dysregulation of innate immunity and pathogenesis of HVI-infected animals [27,28]. In influenza models, activation of type I IFN signaling sensitizes the host to secondary bacterial pneumonia due to impairment of neutrophil responses [29], and potentiates virus-induced apoptosis via the FADD/CASP8 death signaling pathway [30].

The rapid response of the type I IFN pathway in HVI was concurrent with the early expression of the viral dsRNA sensing molecule, RIG-I or DDX58 [31]. However, the earlier expression of IFN-inducible genes in HVI was interestingly accompanied by a modest increase in IFNβ expression. The ability of the influenza virus to suppress IFNβ is likely due to the viral NS1 protein which inhibits IFNβ transcriptional

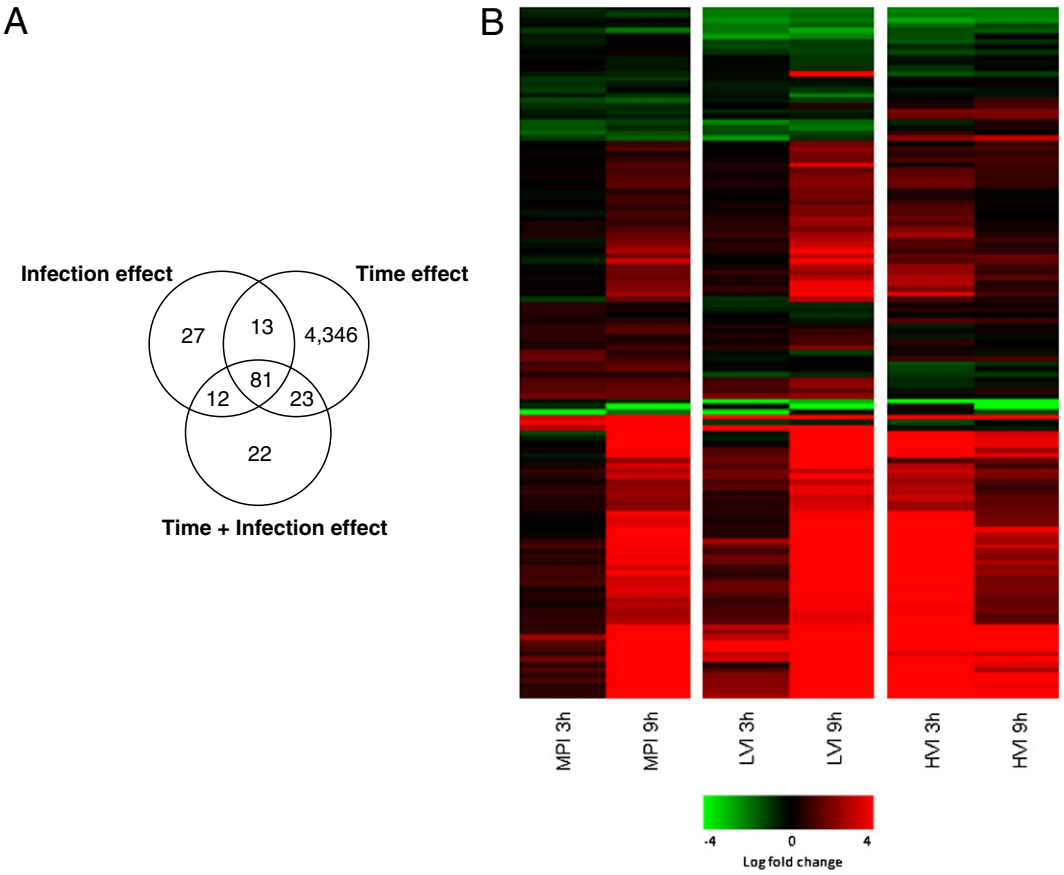
A
Infection effect
Time effect
27
13
4,346
81
12
23
22
Time + Infection effect
B
MPI 3h
MPI 9h
LVI 3h
LVI 9h
HVI 3h
HVI 9h
-4
0
4
Log fold change
C
IRF2
IRF1
ADAR
STAT1
GCH1
CCL5
GBP5
EIF2AK2
DDX58
STAT2
IGTP
IRF9
IRGM2
DHX58
ZBP1
IFIH1
GBP2
IFI202B
GBP4
ISG20
CXCL10
IRF7
ISG15
IFI204
IFI203
GBP3
IFIT1
IFNB1
IFIT3
OASL2
RSAD2
OASL1
IFIT2
MPI 3h
MPI 9h
LVI 3h
LVI 9h
HVI 3h
HVI 9h
-4
0
4
Log fold change

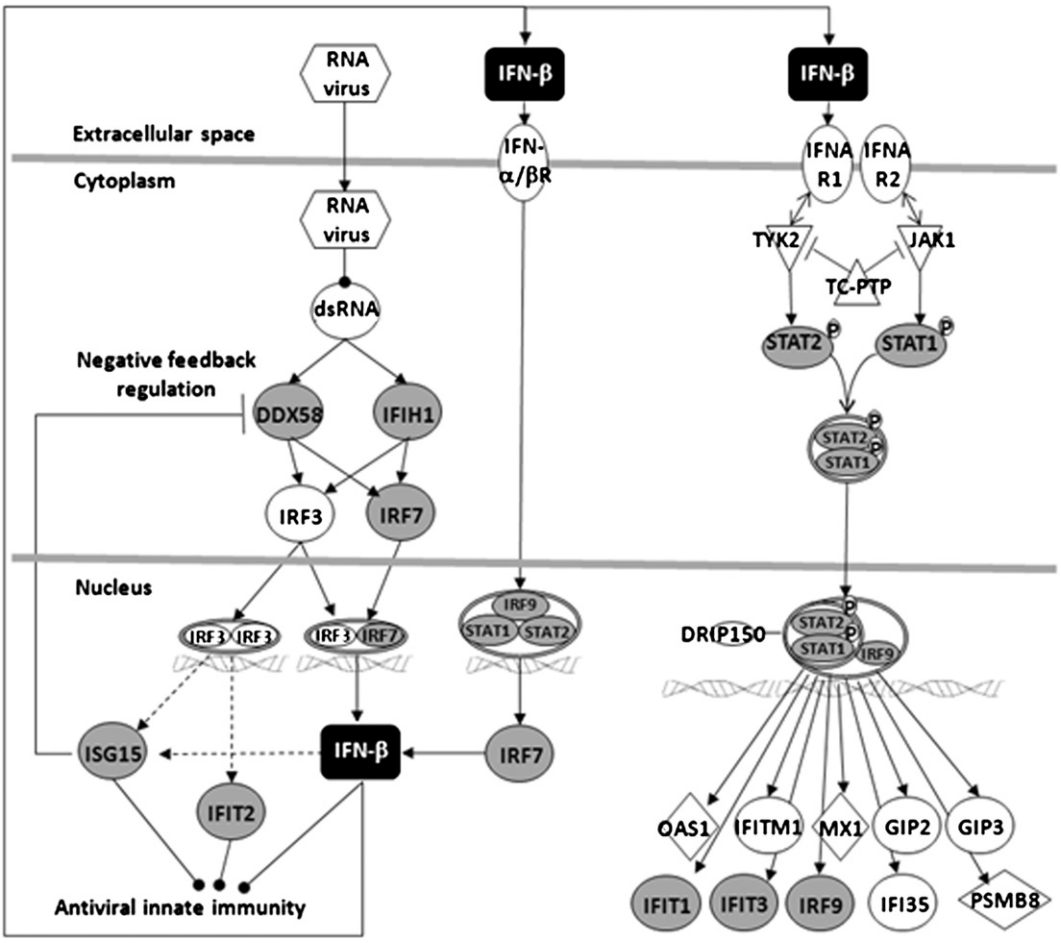

Fig. 6. A sub-network of canonical pathways associated with IFNβ regulation and signaling. Genes that were overexpressed in LVI, HVI, and MPI infections by microarray analyses are shaded gray.

induction via various mechanisms [32,33]. Furthermore, the rapid type I IFN response of neutrophils to HVI virus could not be explained by its higher replication rate alone, since the replication kinetics of HVI and MPI viruses in MDCK cells were similar, but the type I IFN response in MPI infection was relatively slower. Hence, the differences in gene expression kinetics of neutrophils infected by HVI and MPI signify the importance of comparing the original HVI isolate in murine lung homogenate against that propagated in MDCK cells.

The expression levels of several genes encoding cytokines and chemokines were upregulated in neutrophils in response to influenza infection. Of particular interest is CXCL10, an IFNγ-inducible protein that acts as a potent neutrophil chemoattractant [34], and is highly expressed in various animal models of infection with HVI virus. In highly pathogenic H5N1 infection of ferrets, inhibition of CXCR3 (a cognate receptor of CXCL10) reduces lung infiltration and delays mortality [35]. Interestingly, in mice infected with HVI [1], CXCL10 is not elevated, whereas neutrophil chemoattractant CXCL1 (Gro-α or KC) is highly expressed even at 12 h p.i.

In addition, we also demonstrated that influenza virus infection accelerates neutrophil apoptosis. Specifically, the annexin V and TUNEL assays confirmed that MPI-infected neutrophils undergo cell death via apoptosis that was significantly higher than that in uninfected samples, particularly at 6–24 h p.i. These apoptosis findings were complemented by transcriptomic data of infected neutrophils that revealed differential regulation of apoptosis-related genes, including IFN-inducible EIF2AK2 (eukaryotic translation initiation factor 2-alpha kinase 2), and genes involved in retinoic acid-mediated apoptosis signaling. Significantly, HVI triggered more rapid upregulation of these apoptosis-related genes (at 3 h p.i.) in contrast to MPI and LVI (at 9 h p.i.). Influenza-induced neutrophil apoptosis is associated with increased neutrophil expression of Fas antigen and Fas ligand [12]. The respiratory burst may also contribute to reduced neutrophil survival, e.g. after incubation with influenza virus and *Streptococcus pneumoniae* [36]. Neutrophil apoptosis may also be induced by influenza viral proteins, especially the multifunctional NS1 [37]. Hence, abortive influenza virus infection of neutrophils can still induce apoptosis. It is particularly noteworthy that the course of MPI virus-induced neutrophil apoptosis was compatible with the expression of cellular or viral genes, as documented previously [12], and by our experimental data.

Overall, our model of influenza infection using the MPRO cell line has offered new insights into the roles of neutrophils during the pathogenesis of severe influenza. In particular, we propose that the augmented apoptosis and rapid type I IFN responses of HVI-infected neutrophils may contribute to dysregulation of innate immunity in the lungs. It may be worthwhile to investigate neutrophil cell death and gene expression responses to different strains of HVI virus in order to evaluate the contribution of neutrophils to innate immune dysfunction. This model may also be exploited in future studies on the interactions of neutrophils with other related pathogens or diseases. An area of considerable interest would be to explore neutrophil

Fig. 5. Analyses of gene microarray data of influenza infection of neutrophils. (A) Venn diagram showing the overlap between significant groups of genes as analyzed by two-way ANOVA with Benjamini–Hochberg correction for multiple tests. (B) Heatmap of 129 genes with a significant infection effect, and an average absolute log fold change of >0.6 at any time-point of infection with LVI, HVI, and MPI viruses. (C) Heatmap highlighting expression of IFN-related genes in response to infection with LVI, HVI, and MPI.

defects attributed to influenza virus infection, including demonstrating the impact on phagocytosis and developing a secondary bacterial infection model.

4. Materials and methods

4.1. Culture and differentiation of the MPRO cell line into neutrophils

MPRO cells were cultured in Iscove's modified Dulbecco's medium (IMDM) containing 4 mM L-glutamine, 3 g/l sodium bicarbonate, 10 ng/ml murine GM-CSF, and 20% heat-inactivated fetal bovine serum (FBS) at 37 °C with 5% CO_2. The culture medium was replenished in 1–2 days to obtain 5×10^5 cells per ml. To induce the differentiation of MPRO cells into neutrophils, the growth medium was supplemented with 10 μM all-trans retinoic acid. Specific volumes of fresh maintenance medium were added at certain days during differentiation to achieve low or high concentrations of MPRO cells. For excess medium supplementation, an initial 1 vol was added on day 2 after differentiation, 2 vol on day 3, and 1 vol each on days 4 and 5 to attain concentrations of $1–2\times10^5$ cells per ml. Alternatively, limited supplementation of medium was added, i.e. 1.5 vol on day 3, and 0.5 vol each on days 4 and 5. Neutrophil viability was determined based on trypan blue exclusion. For most infection experiments, including microarray analyses, neutrophils were harvested on day 4 or 5 after maintaining with limited medium supplementation.

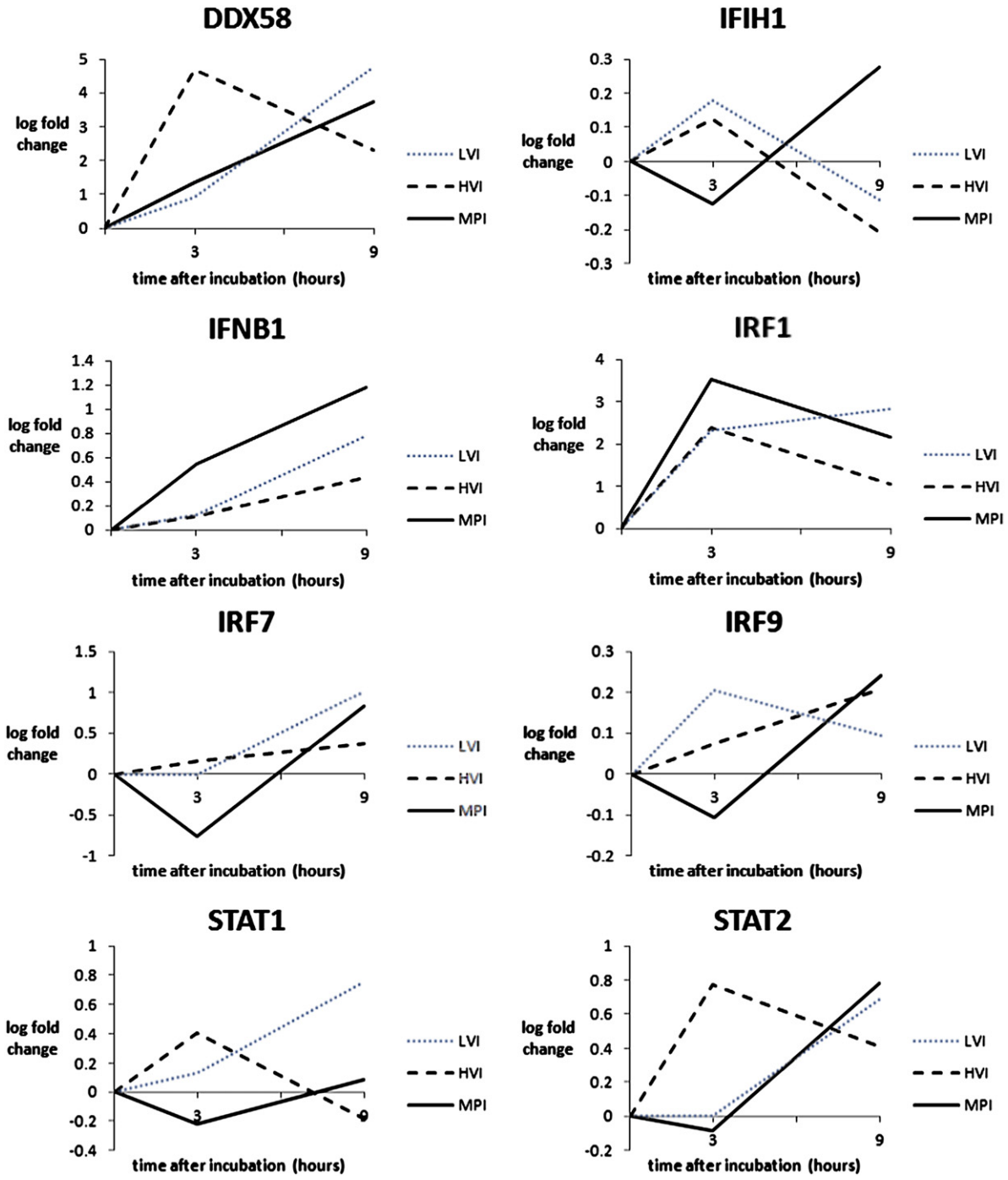

Fig. 7. Validation of microarray data for several IFN-related genes by real-time RT-PCR. Log fold changes (relative to mock control) shown in the graphs reflect the average of duplicate samples.

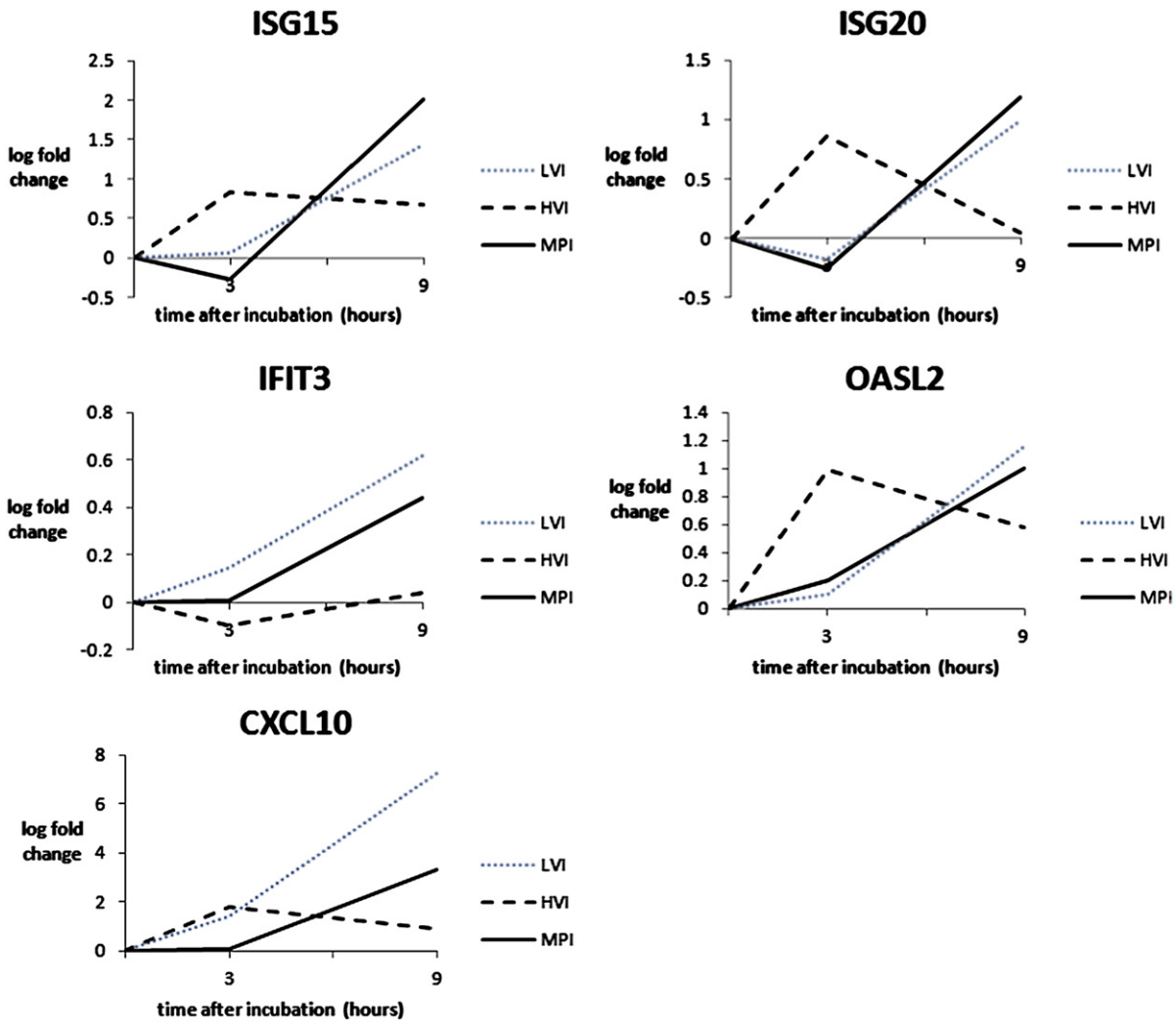

Fig. 7 (*continued*).

4.2. Estimating the proportion of mature neutrophils among the MPRO cell population

The proportion of neutrophils was estimated by flow cytometry of Ly6G-stained MPRO cells, as well as by manual and automated counting of Giemsa-stained neutrophils. For flow cytometry, 10^6 MPRO cells were washed with phosphate-buffered saline (PBS) before and after 20 min incubation at 4 °C with 100 μl of plain stain buffer or buffer containing 1:50 dilution of anti-mouse PerCP-Cy5.5 rat anti-mouse Ly6G (BD Biosciences) or FITC anti-mouse Gr-1 (MACS, Miltenyi Biotec), fixed, and resuspended in sheath buffer. Flow cytometric analysis was performed using the Cytomics FC 500 Series Flow Cytometer (Beckman Coulter), and data were analyzed by the CXP software version 1.0 or WinMDI version 2.9 (Bio-Soft Net). The threshold for singly stained samples was determined by allowing 5% error for their unstained counterparts. The proportion of positively stained cells was obtained by subtracting 5% from the percentage to the right of the threshold of stained samples. For Giemsa staining, 50 μl of each sample containing $2.5–5.0\times10^4$ cells were cyto-centrifuged onto glass slides, subjected to May–Grünwald–Giemsa staining, and scanned by a MIRAX MIDI slide scanner (Carl Zeiss). Ten fields of scanned cells were sampled at 40× magnification, and the neutrophil-like proportion was estimated

Table 1
Changes in expression of genes associated with apoptotic activity in neutrophils infected with influenza viruses. The gene expression changes for MPI, LVI, and HVI infections at the time-points post-infection are expressed as log fold changes.

Gene symbol	Biological activity	MPI		LVI		HVI	
		3 h	9 h	3 h	9 h	3 h	9 h
CASP4	Execution-phase of cell apoptosis	−0.9	1.6	−0.7	2.8	1.2	0.5
EIF2AK2	Inhibition of protein synthesis	0.7	2.7	1.2	3.6	4.2	1.2
NOD1	Enhancement of caspase-9-mediated apoptosis	0.4	0.9	0.6	2.4	1.4	0.4
PARP9	Retinoic acid-mediated apoptosis signaling	0.5	2.3	0.7	3.2	3.2	1.5
PARP10	Retinoic acid-mediated apoptosis signaling	−0.1	1.7	0.4	2.8	2.3	0.9
PARP14	Retinoic acid-mediated apoptosis signaling	0.5	2.6	0.8	4.0	4.1	1.5
RNF34	Anti-apoptotic function	0.0	1.7	0.8	2.3	2.4	0.8
XAF1	Inhibition of anti-caspase activity	1.2	3.9	1.6	5.1	5.0	3.2

manually, or by an automated image analysis system [38]. Smaller images containing fewer cells were randomly cropped without repetition from larger ones for manual counting.

4.3. Virus strains, determination of virus titers, and neutrophil infection

Influenza virus strain A/Aichi/2/68 H3N2 was purchased from the American Type Culture Collection, propagated in eggs, and shown to cause LVI in mice. This virus strain was also adapted to cause HVI in a mouse model through serial lung-to-lung passaging until the tenth passage [27]. For further use, passage 10 HVI virus was passaged using 4–6 week-old female BALB/c mice, where lung homogenates were collected two days after infection. All animal experiments were conducted in a BSL-2 laboratory, and approved by the Institutional Animal Care and Use Committee. HVI virus of the fourteenth passage was used. Since HVI replicates more efficiently than LVI, we also propagated the HVI virus in MDCK cells (termed as "MPI"), and used MPI virus to perform most experiments that analyzed infection of neutrophils. Virus titers were determined either by plaque assay or $TCID_{50}$ assay [27]. For infection, neutrophils were incubated with influenza virus for 1 h at 37 °C with 5% CO_2, and then resuspended in IMDM containing 25 ng/ml GM-CSF to 5×10^6 cells per ml.

4.4. Labeling influenza virus with lipophilic dye for identifying infected cells

Plain EMEM or EMEM containing 10^7 pfu of MPI virus per ml was incubated with 1:20 dilution of the fluorescent lipophilic dye (1,1′-dioctadecyl-3,3,3′,3′-tetramethyl-indodicarbocyanine or DiD) in a 6-well plate for 1 h at 37 °C with 5% CO_2. After incubation, the inocula were filtered using 0.45-μm syringe filters, and frozen at −80 °C until further use. The inoculum without virus but incubated with DiD served as the DiD mock control. Following incubation with DiD-labeled MPI for 1 h, infected cells were identified by flow cytometry or confocal microscopy [39]. For flow cytometry, cells were washed with PBS, stained with FITC Ly6G, fixed, and resuspended in sheath buffer. For confocal microscopy, cells were washed with PBS, cyto-centrifuged onto glass slides, permeabilized with Triton X-100, stained with DAPI, and examined with the Olympus FluoView FV1000 confocal laser scanning microscope using a 100×/1.45 oil objective, with 405 nm solid state laser diode, and 633 nm HeNe laser as the excitation source (for visualizing DiD dye).

4.5. Comparing kinetics of influenza virus replication in MDCK cells and neutrophils

To compare the viral replication kinetics, confluent MDCK cell monolayers in 12-well plates were inoculated with LVI, HVI or MPI virus at MOI of 0.1 (without adding TPCK-treated trypsin), and incubated for 1 h at 37 °C with 5% CO_2. Inocula were removed, replaced with 1 ml of plain EMEM, and 100 μl of each supernatant collected after 3, 6, 12, and 24 h for virus plaque assay. The replication kinetics of MPI in MDCK and neutrophils were compared in 24-well plates. Infected neutrophils were incubated in fresh IMDM containing 25 ng/ml GM-CSF (4×10^6 cells in 800 μl). Supernatants (50 μl each) of both infected cell types were harvested at 6, 12, and 24 h for virus plaque assay.

4.6. Immunofluorescence detection of influenza-infected neutrophils

At 6, 9, 12, and 24 h after infection with MPI virus, $3–5\times10^4$ neutrophils were cyto-centrifuged onto a glass slide. Cells were fixed with formaldehyde, permeabilized with 1% Triton X-100, blocked with 2% FBS and PBS for 10 min and 1 h, respectively. After washing with PBS, cells were incubated overnight with 1:250 dilution of primary rabbit antibody raised against influenza A/Aichi/2/68 H3N2 virus. Cells were then washed twice with PBS, incubated with 1:250 dilution of anti-rabbit Alexa 555 (Molecular Probes) for 1 h in room temperature, washed, and DAPI was applied. Twelve fields of infected neutrophils were captured for analyzing the kinetics of viral protein synthesis using the Olympus BX60 fluorescence microscope. Staining was also performed on neutrophils infected with LVI virus after 9 h and HVI virus after 3 h. Infected MDCK cells stained in a similar way served as positive control.

4.7. Early and late apoptosis assays

Flow cytometry based on annexin V and propidium iodide (PI) staining was performed on 5 replicates of paired uninfected and infected samples collected at 0, 3, 6, 9, 12, and 24 h after incubation with MPI virus. Infected or uninfected neutrophils (1.5×10^6) in 24-well plates were washed with PBS, and incubated with 1:50 dilution of both FITC annexin V and PI (BD Biosciences) in 100 μl of binding buffer for 20 min at room temperature in the dark. Then, 400 μl of binding buffer was added to each sample, cells were gently resuspended, and analyzed by flow cytometry as previously described. TUNEL assay was also performed on cyto-centrifuged samples collected at 12 h after incubation using an In Situ Cell Death detection kit, POD (Roche Applied Science) according to the manufacturer's protocol [40]. The percentage of apoptotic cells was ascertained in a similar way as for the manual neutrophil estimation by Giemsa staining.

4.8. Oligonucleotide microarray experiments

Neutrophils were infected with LVI, HVI (at MOI of 0.1) and MPI virus (at MOI of 1) for 1 h in medium containing 10 ng/ml GM-CSF. The control was represented by neutrophils incubated with uninfected murine lung homogenate (mock infection). Neutrophils were resuspended into 24-well plates (3×10^6 cells per well). After 3 and 9 h of incubation, each supernatant was removed and total RNA was extracted using the RNeasy Mini kit (Qiagen) according to the manufacturer's recommendations. The quantity and purity of total RNA were measured by the Nanodrop ND-100 spectrophotometer, while RNA integrity was verified by the Agilent 2100 Bioanalyzer. Total RNA was labeled with the One Color Low Input Quick Amp labeling kit, version 6.5 (Agilent) following the manufacturer's instructions. Briefly, 100 ng of each RNA sample was converted into double-stranded cDNA with an oligo-dT primer containing the recognition site for T7 RNA polymerase. *In vitro* transcription with T7 RNA polymerase generated cyanine 3-CTP-labeled cRNA. The labeled cRNA (600 ng) was hybridized onto Agilent SurePrint G3 Mouse GE 8×60 K Microarray (design ID 028005) for 17 h at 65 °C, 10 rpm in an Agilent hybridization oven. The microarray slide was then washed in wash buffer 1 for 1 min at room temperature, and another minute in wash buffer 2 at 37 °C before scanning with the Agilent High-Resolution Microarray C Scanner. Raw signal data were extracted from the TIFF image with Agilent Feature Extraction software (version 10.7.1.1).

4.9. Gene microarray data processing and analyses

GeneSpring GX 11.5 (Agilent) was utilized for normalization and filtering of the Agilent microarray data. Percentile shift normalization (set at 75th percentile) was applied on log-transformed data. Baseline transformation to median for each batch of data from each replicate was performed. Batch effect correction was also carried out to correct markers that showed consistent signals within batches but large variations between batches. Probes flagged as detected in any experiment were included in a working list (22,911 transcripts). Two-way ANOVA was applied on this list using R software (http://www.r-project.org/) to identify genes that had significant infection, time, and interaction effects. If a gene had no significant interaction effect, we employed two-way ANOVA without considering the interaction effect to improve the p-value for infection and time effects. The Benjamini–Hochberg

method for multiple test correction implemented in the R software was utilized to adjust p-values of the ANOVA test for each gene. Gene Ontology analysis was performed using FuncAssociate 2.0 [41], while pathway analysis was carried out using Ingenuity Pathway Analysis.

4.10. Quantitative real-time RT-PCR analysis

Total RNA was converted into cDNA using MMLV reverse transcriptase (Promega), and SYBR Green PCR analyses were performed using the LightCycler system (Roche Applied Science) according to the manufacturer's protocol. Primer pairs for selected genes were synthesized based on PrimerBank [42,43], i.e. GAPDH (6679937a1), DDX58 (27370002a1), IRF1 (6680467a1), IRF7 (8567364a1), IRF9 (6680474a1), IFIH1 (23956208a1), STAT1 (27502700a1), STAT2 (9910572a1), IFIT3 (6754288a1), ISG15 (7657240a1), ISG20 (15805028a1), OASL2 (16924024a1), and CXCL10 (10946576a1); except IFNβ primers (5′-CCACAGCCCTCTCCATCAACTATAAGC-3′ and 5′-AGCTCTTCAACTGG AGAGCAGTTGAGG-3′). The uniformity of each amplified product was confirmed by the melting curve displaying a single consistent peak. The GAPDH housekeeping gene was used for normalizing the expression data of other genes. The specificity of each primer pair was confirmed by a single diagnostic band in gel electrophoresis of RT-PCR products.

Acknowledgments

The authors are grateful to S.G. Rozen, S.H. Lau, T. Narasaraju, K.T. Thong, S.Y. Lee, and Y. Teo for their assistance in this project. This study was supported by the Singapore-MIT Alliance. The authors declare no conflict of interest.

References

[1] F.X. Ivan, J.C. Rajapakse, R.E. Welsch, S.G. Rozen, T. Narasaraju, G.M. Xiong, B.P. Engelward, V.T. Chow, Differential pulmonary transcriptomic profiles in murine lungs infected with low and highly virulent influenza H3N2 viruses reveal dysregulation of TREM1 signaling, cytokines, and chemokines, Funct. Integr. Genomics 12 (2012) 105–117.
[2] L.A. Perrone, J.K. Plowden, A. Garcia-Sastre, J.M. Katz, T.M. Tumpey, H5N1 and 1918 pandemic influenza virus infection results in early and excessive infiltration of macrophages and neutrophils in the lungs of mice, PLoS Pathog. 4 (2008) e1000115.
[3] S.M. Lee, J.L. Gardy, C.Y. Cheung, T.K. Cheung, K.P. Hui, N.Y. Ip, Y. Guan, R.E. Hancock, J.S. Peiris, Systems-level comparison of host-responses elicited by avian H5N1 and seasonal H1N1 influenza viruses in primary human macrophages, PLoS One 4 (2009) e8072.
[4] G. Zinman, R. Brower-Sinning, C.H. Emeche, J. Ernst, G.T. Huang, S. Mahony, A.J. Myers, D.M. O'Dee, J.L. Flynn, G.J. Nau, T.M. Ross, R.D. Salter, P.V. Benos, Z. Bar Joseph, P.A. Morel, Large scale comparison of innate responses to viral and bacterial pathogens in mouse and macaque, PLoS One 6 (2011) e22401.
[5] W.C. Yu, R.W. Chan, J. Wang, E.A. Travanty, J.M. Nicholls, J.S. Peiris, R.J. Mason, M.C. Chan, Viral replication and innate host responses in primary human alveolar epithelial cells and alveolar macrophages infected with influenza H5N1 and H1N1 viruses, J. Virol. 85 (2011) 6844–6855.
[6] M.D. Tate, L.J. Ioannidis, B. Croker, L.E. Brown, A.G. Brooks, P.C. Reading, The role of neutrophils during mild and severe influenza virus infections of mice, PLoS One 6 (2011) e17618.
[7] T. Narasaraju, E. Yang, R.P. Samy, H.H. Ng, W.P. Poh, A.A. Liew, M.C. Phoon, N. van Rooijen, V.T. Chow, Excessive neutrophils and neutrophil extracellular traps contribute to acute lung injury of influenza pneumonitis, Am. J. Pathol. 179 (2011) 199–210.
[8] K.L. Hartshorn, L.S. Liou, M.R. White, M.M. Kazhdan, J.L. Tauber, A.I. Tauber, Neutrophil deactivation by influenza A virus. Role of hemagglutinin binding to specific sialic acid-bearing cellular proteins, J. Immunol. 154 (1995) 3952–3960.
[9] L.F. Cassidy, D.S. Lyles, J.S. Abramson, Synthesis of viral proteins in polymorphonuclear leukocytes infected with influenza A virus, J. Clin. Microbiol. 26 (1988) 1267–1270.
[10] R.M. Lee, M.R. White, K.L. Hartshorn, Influenza A viruses upregulate neutrophil toll-like receptor 2 expression and function, Scand. J. Immunol. 63 (2006) 81–89.
[11] J.P. Wang, G.N. Bowen, C. Padden, A. Cerny, R.W. Finberg, P.E. Newburger, E.A. Kurt-Jones, Toll-like receptor-mediated activation of neutrophils by influenza A virus, Blood 112 (2008) 2028–2034.
[12] M.L. Colamussi, M.R. White, E. Crouch, K.L. Hartshorn, Influenza A virus accelerates neutrophil apoptosis and markedly potentiates apoptotic effects of bacteria, Blood 93 (1999) 2395–2403.
[13] P. Gaines, J. Chi, N. Berliner, Heterogeneity of functional responses in differentiated myeloid cell lines reveals EPRO cells as a valid model of murine neutrophil functional activation, J. Leukoc. Biol. 77 (2005) 669–679.
[14] C.L. Liu, S. Tangsombatvisit, J.M. Rosenberg, G. Mandelbaum, E.C. Gillespie, O.P. Gozani, A.A. Alizadeh, P.J. Utz, Specific post-translational histone modifications of neutrophil extracellular traps as immunogens and potential targets of lupus autoantibodies, Arthritis Res. Ther. 14 (2012) R25.
[15] D. Ermert, C.F. Urban, B. Laube, C. Goosmann, A. Zychlinsky, V. Brinkmann, Mouse neutrophil extracellular traps in microbial infections, J. Innate Immun. 1 (2009) 181–193.
[16] T.J. Fleming, M.L. Fleming, T.R. Malek, Selective expression of Ly-6G on myeloid lineage cells in mouse bone marrow. RB6-8C5 mAb to granulocyte-differentiation antigen (Gr-1) detects members of the Ly-6 family, J. Immunol. 151 (1993) 2399–2408.
[17] J.M. Daley, A.A. Thomay, M.D. Connolly, J.S. Reichner, J.E. Albina, Use of Ly6G-specific monoclonal antibody to deplete neutrophils in mice, J. Leukoc. Biol. 83 (2008) 64–70.
[18] B.S. Johnson, R.A. Chandraratna, R.A. Heyman, E.A. Allegretto, L. Mueller, S.J. Collins, Retinoid X receptor (RXR) agonist-induced activation of dominant-negative RXR-retinoic acid receptor alpha403 heterodimers is developmentally regulated during myeloid differentiation, Mol. Cell. Biol. 19 (1999) 3372–3382.
[19] M. Lakadamyali, M.J. Rust, H.P. Babcock, X. Zhuang, Visualizing infection of individual influenza viruses, Proc. Natl. Acad. Sci. U. S. A. 100 (2003) 9280–9285.
[20] J. Yin, T.A. Ferguson, Identification of an IFN-gamma-producing neutrophil early in the response to *Listeria monocytogenes*, J. Immunol. 182 (2009) 7069–7073.
[21] T. Matsumura, M. Ato, T. Ikebe, M. Ohnishi, H. Watanabe, K. Kobayashi, Interferon-γ-producing immature myeloid cells confer protection against severe invasive group A *Streptococcus* infections, Nat. Commun. 3 (2012) 678.
[22] S. Nance, R. Cross, A.K. Yi, E.A. Fitzpatrick, IFN-gamma production by innate immune cells is sufficient for development of hypersensitivity pneumonitis, Eur. J. Immunol. 35 (2005) 1928–1938.
[23] D. Lindau, A. Rabsteyn, I. Kötter, A. Igney, M.C. Boissier, H.G. Rammensee, P. Decker, Chromatin-activated neutrophils represent a major source of interferon α, Ann. Rheum. Dis. 70 (2011) A38–A39.
[24] S. Martinelli, M. Urosevic, A. Daryadel, P.A. Oberholzer, C. Baumann, M.F. Fey, R. Dummer, H.U. Simon, S. Yousefi, Induction of genes mediating interferon-dependent extracellular trap formation during neutrophil differentiation, J. Biol. Chem. 279 (2004) 44123–44132.
[25] M.P. Berry, C.M. Graham, F.W. McNab, Z. Xu, S.A. Bloch, T. Oni, K.A. Wilkinson, R. Banchereau, J. Skinner, R.J. Wilkinson, C. Quinn, D. Blankenship, R. Dhawan, J.J. Cush, A. Mejias, O. Ramilo, O.M. Kon, V. Pascual, J. Banchereau, D. Chaussabel, A. O'Garra, An interferon-inducible neutrophil-driven blood transcriptional signature in human tuberculosis, Nature 466 (2010) 973–977.
[26] I. Koerner, G. Kochs, U. Kalinke, S. Weiss, P. Staeheli, Protective role of beta interferon in host defense against influenza A virus, J. Virol. 81 (2007) 2025–2030.
[27] T. Narasaraju, M.K. Sim, H.H. Ng, M.C. Phoon, N. Shanker, S.K. Lal, V.T. Chow, Adaptation of human influenza H3N2 virus in a mouse pneumonitis model: insights into viral virulence, tissue tropism and host pathogenesis, Microbes Infect. 11 (2009) 2–11.
[28] H.H. Ng, T. Narasaraju, M.C. Phoon, M.K. Sim, J.E. Seet, V.T. Chow, Doxycycline treatment attenuates acute lung injury in mice infected with virulent influenza H3N2 virus: involvement of matrix metalloproteinases, Exp. Mol. Pathol. 92 (2012) 287–295.
[29] A. Shahangian, E.K. Chow, X. Tian, J.R. Kang, A. Ghaffari, S.Y. Liu, J.A. Belperio, G. Cheng, J.C. Deng, Type I IFNs mediate development of postinfluenza bacterial pneumonia in mice, J. Clin. Invest. 119 (2009) 1910–1920.
[30] S. Balachandran, P.C. Roberts, T. Kipperman, K.N. Bhalla, R.W. Compans, D.R. Archer, G.N. Barber, Alpha/beta interferons potentiate virus-induced apoptosis through activation of the FADD/Caspase-8 death signaling pathway, J. Virol. 74 (2000) 1513–1523.
[31] Y.M. Loo, J. Fornek, N. Crochet, G. Bajwa, O. Perwitasari, L. Martinez-Sobrido, S. Akira, M.A. Gill, A. Garcia-Sastre, M.G. Katze, M. Gale, Distinct RIG-I and MDA5 signaling by RNA viruses in innate immunity, J. Virol. 82 (2008) 335–345.
[32] M.U. Gack, R.A. Albrecht, T. Urano, K.S. Inn, I.C. Huang, E. Carnero, M. Farzan, S. Inoue, J.U. Jung, A. Garcia-Sastre, Influenza A virus NS1 targets the ubiquitin ligase TRIM25 to evade recognition by the host viral RNA sensor RIG-I, Cell Host Microbe 5 (2009) 439–449.
[33] K.S. Tan, F. Olfat, M.C. Phoon, J.P. Hsu, J.L. Howe, J.E. Seet, K.C. Chin, V.T. Chow, In vivo and in vitro studies on the antiviral activities of viperin against influenza H1N1 virus infection, J. Gen. Virol. 93 (2012) 1269–1277.
[34] L. Michalec, B.K. Choudhury, E. Postlethwait, J.S. Wild, R. Alam, M. Lett-Brown, S. Sur, CCL7 and CXCL10 orchestrate oxidative stress-induced neutrophilic lung inflammation, J. Immunol. 168 (2002) 846–852.
[35] C.M. Cameron, M.J. Cameron, J.F. Bermejo-Martin, L. Ran, L. Xu, P.V. Turner, R. Ran, A. Danesh, Y. Fang, P.K. Chan, N. Mytle, T.J. Sullivan, T.L. Collins, M.G. Johnson, J.C. Medina, T. Rowe, D.J. Kelvin, Gene expression analysis of host innate immune responses during lethal H5N1 infection in ferrets, J. Virol. 82 (2008) 11308–11317.
[36] G. Engelich, M. White, K.L. Hartshorn, Neutrophil survival is markedly reduced by incubation with influenza virus and *Streptococcus pneumoniae*: role of respiratory burst, J. Leukoc. Biol. 69 (2001) 50–56.

[37] B.G. Hale, R.E. Randall, J. Ortin, D. Jackson, The multifunctional NS1 protein of influenza A viruses, J. Gen. Virol. 89 (2008) 2359–2376.
[38] F.X. Ivan, R.E. Welsch, V.T. Chow, J.C. Rajapakse, Estimation of the population of neutrophils induced to differentiate from the MPRO mouse promyelocytic cell line, in: Conf. Proc. IEEE Eng. Med. Biol. Soc, 2011, pp. 6001–6004.
[39] D.L. Sim, V.T. Chow, The novel human HUEL (C4orf1) gene maps to chromosome 4p12-p13 and encodes a nuclear protein containing the nuclear receptor interaction motif, Genomics 59 (1999) 224–233.
[40] K.M. Lim, V.T. Chow, Induction of marked apoptosis in mammalian cancer cell lines by antisense DNA treatment to abolish expression of DENN (differentially expressed in normal and neoplastic cells), Mol. Carcinog. 35 (2002) 110–126.
[41] G.F. Berriz, J.E. Beaver, C. Cenik, M. Tasan, F.P. Roth, Next generation software for functional trend analysis, Bioinformatics 25 (2009) 3043–3044.
[42] A. Spandidos, X. Wang, H. Wang, B. Seed, PrimerBank: a resource of human and mouse PCR primer pairs for gene expression detection and quantification, Nucleic Acids Res. 38 (2010) D792–D799.
[43] X. Wang, A. Spandidos, H. Wang, B. Seed, PrimerBank: a PCR primer database for quantitative gene expression analysis, 2012 update, Nucleic Acids Res. 40 (2012) D1144–D1149.